Hindawi Publishing Corporation
Mathematical Problems in Engineering
Volume 2015, Article ID 180841, 8 pages
http://dx.doi.org/10.1155/2015/180841

Research Article

Numerical Study of Laminar Flow Forced Convection of Water-Al_2O_3 Nanofluids under Constant Wall Temperature Condition

Hsien-Hung Ting and Shuhn-Shyurng Hou

Department of Mechanical Engineering, Kun Shan University, Tainan City 71070, Taiwan

Correspondence should be addressed to Shuhn-Shyurng Hou; sshou@mail.ksu.edu.tw

Received 28 September 2014; Accepted 11 December 2014

Academic Editor: Mo Li

This numerical study is aimed at investigating the forced convection heat transfer and flow characteristics of water-based Al_2O_3 nanofluids inside a horizontal circular tube in the laminar flow regime under the constant wall temperature boundary condition. Five volume concentrations of nanoparticle, 0.1, 0.5, 1, 1.5, and 2 vol.%, are used and diameter of nanoparticle is 40 nm. Characteristics of heat transfer coefficient, Nusselt number, and pressure drop are reported. The results show that heat transfer coefficient of nanofluids increases with increasing Reynolds number or particle volume concentration. The heat transfer coefficient of the water-based nanofluid with 2 vol.% Al_2O_3 nanoparticles is enhanced by 32% compared with that of pure water. Increasing particle volume concentration causes an increase in pressure drop. At 2 vol.% of particle concentration, the pressure drop reaches a maximum that is nearly 5.7 times compared with that of pure water. It is important to note that the numerical results are in good agreement with published experimental data.

1. Introduction

Nanofluids are advanced heat transfer fluids containing nanosized particles (typically 1 to 100 nm) dispersed in a conventional liquid, such as water, engine oil, and ethylene glycol. It is well recognized that thermal conductivity of solids is greater than liquids. Thus, the addition of nanoparticles, generally a metal or metal oxide, in a fluid can greatly improve the thermal conductivity of liquids and in turn increase conduction as well as convection coefficients. As expected, these suspended nanoparticles can significantly change the transport and thermal properties of the conventional liquid (base fluid) since nanofluids have substantial higher thermal conductivities compared to the base fluids. The considerable enhancement of forced convection heat transfer has been widely studied in alumina-water-, TiO_2-water-, and CuO-water-based experimental systems [1–7].

Heyhat et al. [6] experimentally investigated the characteristics of laminar convective heat transfer and pressure drop of Al_2O_3-water nanofluid under constant wall temperature condition. It was found that the heat transfer coefficient of nanofluid was higher than base fluid (water) and that heat transfer enhancement increased with an increase in Reynolds number and particle concentrations.

Wen and Ding [7] studied laminar flow heat transfer of water-based Al_2O_3 nanofluids flowing through a circular pipe. Their results showed that heat transfer enhancement was increased by increasing the nanoparticle concentration at constant Reynolds number. Subsequently, Heris et al. [8, 9] experimentally and numerically investigated the forced convection heat transfer of water-based oxide (CuO and Al_2O_3) nanofluids in a circular tube under constant wall temperature condition. Their results also showed that increasing the particle concentration increased the heat transfer augmentation.

Mirmasoumi and Behzadmehr [10] used two-phase mixture model to numerically study the effect of the size of nanoparticles on mixed convection heat transfer of water-based Al_2O_3 nanofluids. It was found that when decreasing

the nanoparticles mean diameter, the convection heat transfer coefficient significantly increased.

Sharma et al. [11] investigated the enhancement of convective heat transfer using water-based Al_2O_3 nanofluids at various Reynolds numbers under constant wall heat flux boundary condition. Their results showed that considerable enhancement of convective heat transfer was found for nanofluids compared to flow with base fluid (water). It was also found that Reynolds number increment increased convective heat transfer.

A lot of experimental and numerical researches have been performed on the heat transfer enhancement of nanofluids compared to base fluid. In most studies, the constant wall heat flux condition was applied [12–17]. However, there is still a lack of studies on convective heat transfer of nanofluids under the constant wall temperature condition. Therefore, in this study, we aim to numerically investigate the forced convection heat transfer and flow characteristics of water-based Al_2O_3 nanofluids flowing through a horizontal circular tube in the laminar flow regime under the constant wall temperature boundary condition. The nanoparticle size is set equal to 40 nm and five particle concentrations of 0.1, 0.5, 1, 1.5, and 2 vol.% are considered. Furthermore, the effect of Reynolds number on convective heat transfer coefficient and pressure drop is investigated and the results are compared with those of Heyhat et al.'s study [6].

2. Theoretical Model

In the present study, the single-phase approach, which has been used frequently for nanofluids, is adopted. It is assumed that the fluid phase and particles are in thermal equilibrium and move with the same velocity considering the ultrafine (40 nm) and low volume fraction (≤2 vol.%) of the solid particles.

The following governing equations represent the mathematical formulation of the single-phase model, which includes conservation of mass, momentum, and energy for the flow inside the tube:

(i) conservation of mass,

$$\operatorname{div}\left(\rho_{\mathrm{nf}}\vec{V}\right) = 0, \tag{1}$$

(ii) conservation of momentum,

$$\operatorname{div}\left(\rho_{\mathrm{nf}}\vec{V}\vec{V}\right) = -\nabla P + \mu_{\mathrm{nf}}\nabla^2\vec{V}, \tag{2}$$

(iii) conservation of energy,

$$\operatorname{div}\left(\rho_{\mathrm{nf}}\vec{V}C_{\mathrm{nf}}T\right) = \operatorname{div}\left(k_{\mathrm{nf}}\nabla T\right). \tag{3}$$

In the above equations, $\vec{V}$, P, and T are, respectively, fluid velocity vector, pressure, and temperature; ρ, μ, k, and C are density, dynamic viscosity, thermal conductivity, and specific heat capacity, respectively; subscript nf represents nanofluid property. All fluid properties are calculated at the reference temperature (i.e., the fluid inlet temperature $T_{b,i}$).

The physical properties of nanofluid, including density, thermal conductivity, and viscosity, are evaluated as follows.

(i) Density of Nanofluid. Density of nanofluid can be calculated from the mixing theory (Pak and Cho [4]); that is,

$$\rho_{\mathrm{nf}} = (1-\phi)\,\rho_{\mathrm{bf}} + \phi\rho_p. \tag{4}$$

(ii) Specific Heat Capacity C_{nf} of Nanofluid. It is assumed that the Al_2O_3 nanoparticles and the water (base fluid) are in thermal equilibrium. Hence, specific heat capacity C_{nf} of nanofluid can be predicted by (5) (Xuan and Roetzel [5]) as follows:

$$C_{\mathrm{nf}} = \frac{(1-\phi)\,(\rho C)_{\mathrm{nf}} + \phi\,(\rho C)_p}{\rho_{\mathrm{nf}}}. \tag{5}$$

(iii) Effective Thermal Conductivity of Nanofluid. Effective thermal conductivity of nanofluid can be calculated from the following empirical equation (Heyhat et al. [6]) based on the curve fit for the experimental data of thermal conductivity; that is,

$$k_{\mathrm{nf}} = (8.733\phi + 1)\,k_{\mathrm{bf}}. \tag{6}$$

(iv) Viscosity of Nanofluid. Viscosity of Al_2O_3-water nanofluid can also be calculated from Heyhat et al.'s empirical equation [6]; namely,

$$\mu_{\mathrm{nf}} = \left[\exp\left(\frac{5.989\phi}{0.287-\phi}\right)\right]\mu_{\mathrm{bf}}. \tag{7}$$

The empirical correlating equations for predicting the effective thermal conductivity and viscosity of Al_2O_3-water nanofluids are valid for the temperature in the range from 20 to 60°C and particle volume concentration ranging from 0.1 to 2.0 vol.%. Table 1 presents how the transport properties vary with nanoparticle volume fraction using the empirical correlating equations (4)–(7).

Additionally, the physical properties of Al_2O_3 nanoparticle are k_p (thermal conductivity) = 42.34 W/m°C, ρ_p (density) = 3900 kg/m^3, and C_p (specific heat capacity) = 880 J/kg°C, which can be found in [18].

Water-based Al_2O_3 nanofluids with various volume fractions (0.1, 0.5, 1, 1.5, and 2 vol.%) are used as input fluids. For comparison purposes, water is also employed. The convective heat transfer coefficient and pressure drop are investigated for various Reynolds numbers in the range of 360 < Re < 2100. Boundary conditions are specified as follows.

The boundary conditions in the simulation are the same as those in Heyhat et al.'s study [6]. In literature [6], first the flow passed an insulated 50 cm long copper tube, which is sufficiently long for the laminar flow to be fully developed at the inlet of the test section. Therefore, at the inlet of computational domain, hydrodynamically fully developed velocity profile for laminar flow is used, and uniform temperature

Table 1: Thermophysical properties of Al_2O_3-water nanofluid.

Property	T (°C)	Volume concentration (%)					
		0.0	0.1	0.5	1.0	1.5	2.0
ρ (kg/m^3)	20	998.3	1001.20	1012.81	1027.32	1041.83	1056.3
	40	992.3	995.21	1006.84	1021.38	1035.92	1050.5
	60	983.1	986.02	997.69	1012.27	1026.85	1041.4
C (J/kg-°C)	20	4182	4169.1	4118.4	4056.7	3996.6	3938.2
	40	4179	4166.1	4115.1	4053.0	3992.7	3934.0
	60	4186	4172.9	4121.4	4058.6	3997.7	3938.4
μ (mPa s)	20	1.003	1.0249	1.1193	1.2542	1.4114	1.5956
	40	0.653	0.6673	0.7287	0.8165	0.9189	1.0388
	60	0.466	0.4762	0.5200	0.58270	0.6557	0.7413
k (W/m-K)	20	0.5996	0.6048	0.6258	0.6520	0.6781	0.7043
	40	0.6286	0.6341	0.6561	0.6835	0.7109	0.7384
	60	0.6507	0.6564	0.6791	0.7075	0.7359	0.7644

inlet boundary condition ($T_{b,i}$) is specified. At the outlet, the fully developed conditions prevail; in other words all axial derivatives are zero. Additionally, no-slip conditions and constant wall temperature (100°C) are imposed on the tube wall.

A Computational Fluid Dynamics (CFD) code (FLUENT) is used to solve governing equations of laminar force convection heat transfer in horizontal circular tube with constant wall temperature by means of a finite volume method. Figure 1 shows the geometrical configuration used in the simulation. It is a 2.0 m long horizontal tube with 0.005 m inner diameter and is exactly the same as that used in Heyhat et al.'s experiment [6]. GAMBIT model is employed to describe problem which graphs and meshes the spatial domain with size of 2000 × 20, 2000 with length of pipe and 20 with radius.

Numerical simulation is carried out at various Reynolds numbers and particle concentrations (0.1, 0.5, 1, 1.5, and 2 vol.%). The particle size is 40 nm. During the simulation, the residuals of the algebraic discretized equations, resulting from the spatial integration of the conservation equations over finite control volumes, are monitored. Converged solutions are obtained when the residuals for all discretized equations are lower than 10^{-6}. Then heat transfer coefficient, Nusselt number, and friction factor are calculated using the following equations [19]:

$$\overline{h_{\mathrm{nf}}} = \frac{C_{\mathrm{nf}}\rho_{\mathrm{nf}}\overline{U}A\left(T_{b,o}-T_{b,i}\right)}{\pi DL\left(T_w-T_b\right)_{\mathrm{LMTD}}}$$

$$\overline{\mathrm{Nu}_{\mathrm{nf}}} = \frac{\overline{h_{\mathrm{nf}}}D}{K} \tag{8}$$

$$f_{\mathrm{nf}} = \frac{2D\Delta P_{\mathrm{nf}}}{\overline{U}^2\rho_{\mathrm{nf}}L},$$

where $\overline{h_{\mathrm{nf}}}$, $\overline{\mathrm{Nu}_{\mathrm{nf}}}$, and f_{nf} are the average heat transfer coefficient, Nusselt number, and friction factor of the nanofluid, respectively, L is the tube length, D is the tube diameter (inner diameter), $\overline{U}$ is the mean flow velocity, $(T_w - T_b)_{\mathrm{LMTD}}$ is the logarithmic mean temperature difference, T_w is the average tube wall temperature, T_b is the bulk (mean) temperature, also, $T_{b,i}$ and $T_{b,o}$ are the inlet and outlet bulk (mean) temperature, and ΔP_{nf} is the pressure drop.

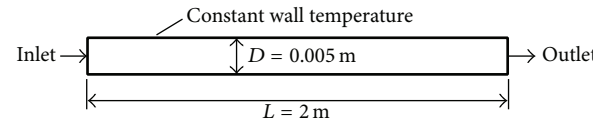

Figure 1: Geometrical configuration in the simulation.

3. Results and Discussion

At first, base fluid (water) is adopted in the CFD simulation for the verification of the numerical method by the comparisons of Nusselt numbers and pressure drops for the fully developed flow condition in a tube. Figure 2 shows the comparison of results as obtained for the average Nusselt number with others' experimental data (Heyhat et al. [6]) and theoretical solutions (Incroprea et al. [19]) in the fully developed laminar regime. Equation (9) [19] shows the correlation for average Nusselt number in the fully developed laminar regime under the constant wall temperature condition. As can be seen, the present numerical results coincide with the experiment [6] and theory [19]:

$$\overline{\mathrm{Nu}} = 3.66 + \frac{0.0688\,(D/L)\,\mathrm{RePr}}{1 + 0.04\left[(D/L)\,\mathrm{RePr}\right]^{2/3}}. \tag{9}$$

Figure 3 presents the pressure drop as a function of Reynolds number for a comparison of the present numerical results, experimental data [6], and theoretical predictions (Hagen-Poiseuille Law, given by (10)). Figure 3 indicates that the present numerical results are in good agreement with the

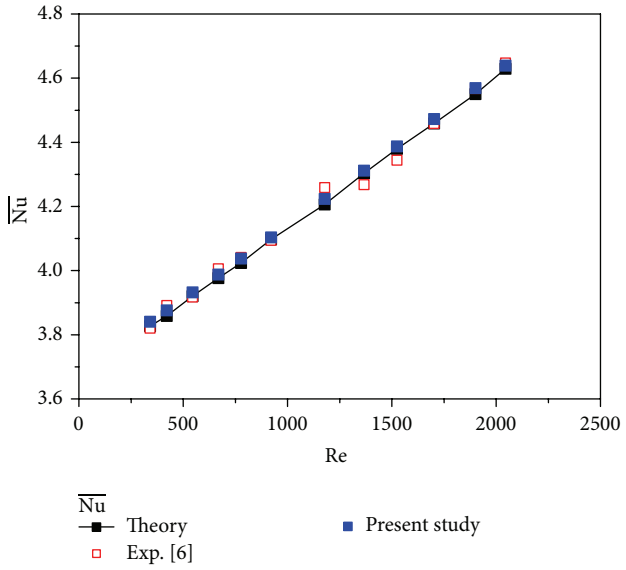

Figure 2: Variations of Nusselt number with Reynolds number for base fluid (water): comparison among present numerical results, experimental data [6], and theoretical solution calculated by (9) [19].

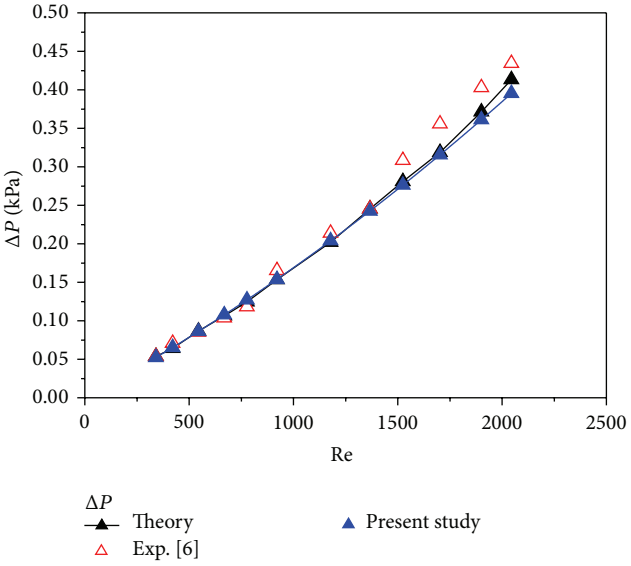

Figure 3: Variations of pressure drop with Reynolds number for base fluid (water): comparison among present numerical results, experimental data [6], and theoretical solution (Hagen-Poiseuille Law) using (10).

experimental results [6] and theoretical analysis calculated using

$$\Delta P = \frac{32\mu L\overline{U}}{D^2}. \tag{10}$$

Figure 4 shows the numerical prediction for the nanofluid-to-water ratio ($\overline{h}/\overline{h_w}$) of average convective heat transfer coefficients versus particle volume concentration (ϕ) at various Reynolds numbers (Re). As can be noticed, significant increases of the average heat transfer coefficient

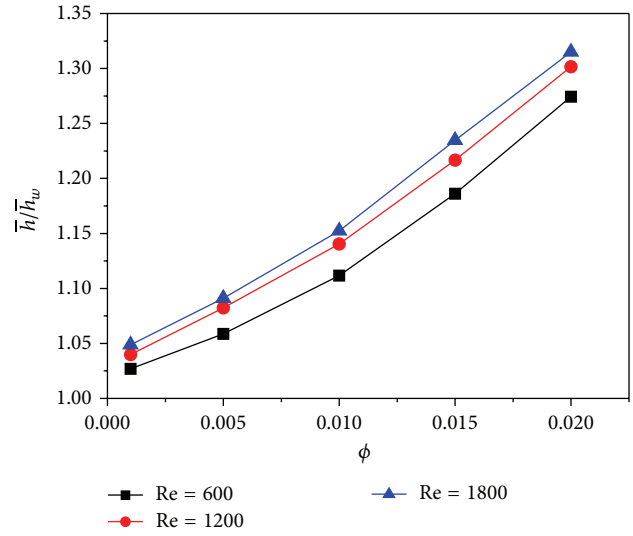

Figure 4: Variations of nanofluid-to-water ratio of average heat transfer coefficient ($\overline{h}/\overline{h_w}$) with particle volume concentration (ϕ) for different values of Reynolds number (Re): present numerical results.

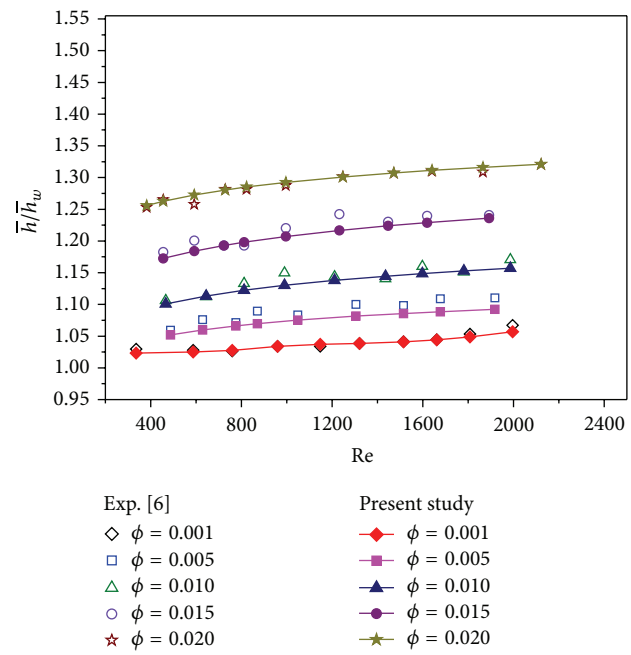

Figure 5: Variations of nanofluid-to-water ratio of average heat transfer coefficient ($\overline{h}/\overline{h_w}$) with Reynolds number (Re) for different values of particle volume concentration (ϕ): comparison between present numerical results and experimental data [6].

are found with the use of nanofluids. Also, it is found that the average heat transfer coefficient increases with Reynolds number for a fixed particle volume concentration.

Figure 5 demonstrates the comparison between the present numerical results and experimental data [6] for the nanofluid-to-water ratio ($\overline{h}/\overline{h_w}$) of average convective heat transfer coefficients as a function of Reynolds number and

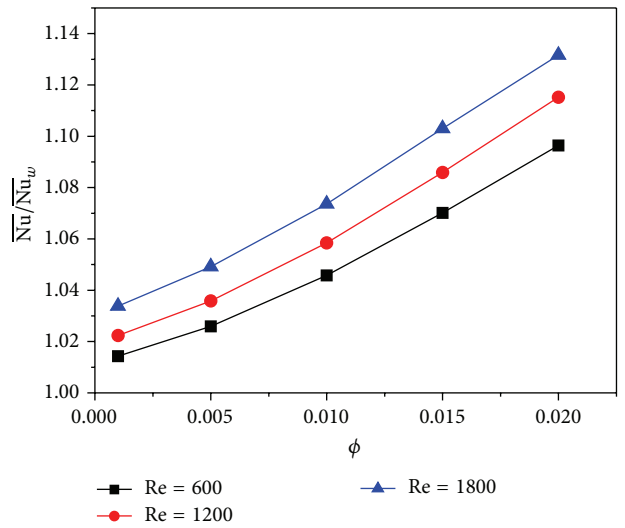

Figure 6: Variations of nanofluid-to-water ratio of average Nusselt number ($\overline{Nu}/\overline{Nu}_w$) with particle volume concentration (ϕ) for different values of Reynolds number (Re): present numerical results.

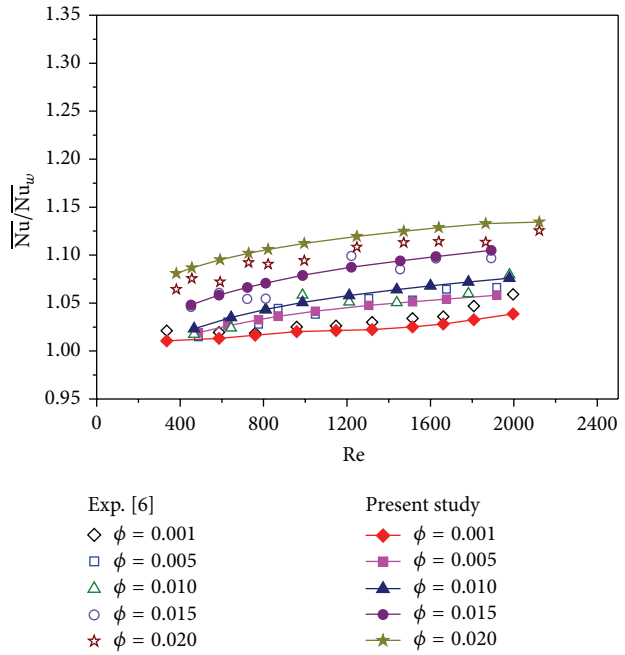

Figure 7: Variations of nanofluid-to-water ratio of average Nusselt number ($\overline{Nu}/\overline{Nu}_w$) with Reynolds number (Re) for different values of particle volume concentration (ϕ): comparison between present numerical results and experimental data [6].

particle volume concentration. It can be noted that better heat transfer characteristics for nanofluids are found compared to distilled water. That is, the heat transfer coefficient of nanofluid increases by increasing the nanoparticle concentration. As can be found, at Re = 2100, the heat transfer coefficient of the water-based Al_2O_3 nanofluid with ϕ = 2 vol.% is enhanced by 32% compared with that of pure water. Also, it can be seen from (6) and (7) (or Table 1), at

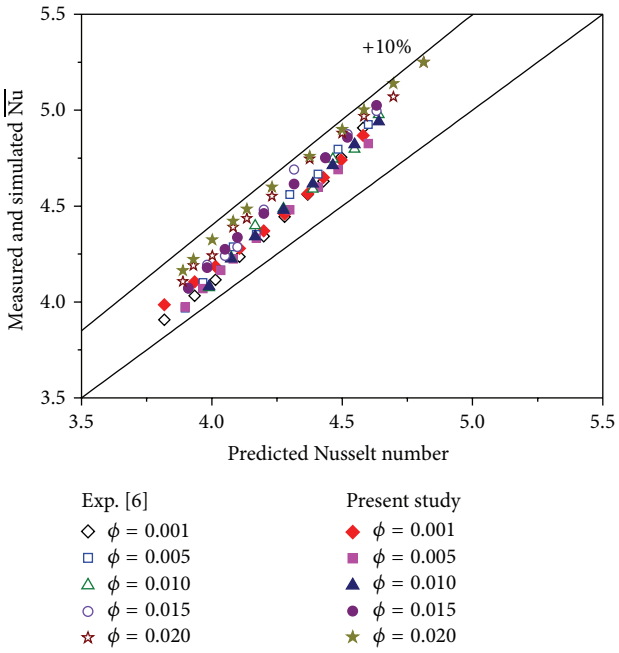

Figure 8: Nusselt number ($\overline{Nu}$) comparison among the present numerical results, experimental data [6], and theoretical prediction using (9) [19] for different values of particle volume concentration (ϕ).

ϕ = 2 vol.%, that the increase of the thermal conductivity and viscosity is approximately 17% and 59%, respectively. Notably, as shown in this work and Heyhat et al.'s study [6], if compared at the same Reynolds number, the heat transfer coefficients of nanofluids relative to that of base fluid (water) increase more due to increased viscosity than due to enhanced thermal conductivity. Moreover, the convective heat transfer coefficient is enhanced with increasing Reynolds number for a constant particle volume concentration. It can be seen from Figures 4 and 5 that the heat transfer coefficient of Al_2O_3-water increases with increase of volume concentration and Reynolds number. This is attributed to the influence of particle Brownian motion and microconvection of the nanoparticles in the base fluid [17].

Figure 6 shows the numerical prediction for the nanofluid-to-water ratio ($\overline{Nu}/\overline{Nu}_w$) of average Nusselt number versus particle volume concentration at various Reynolds numbers. As can be seen, the presence of nanoparticles has considerable effects on the heat transfer characteristics of the mixture. For a given Reynolds number, an increase in the average Nusselt number is observed with the use of nanofluids. It is also found that the average Nusselt number increases with Reynolds number for a constant particle volume concentration.

Figure 7 demonstrates the comparison between the present numerical results and experimental data [6] for the nanofluid-to-water ratio ($\overline{Nu}/\overline{Nu}_w$) of average Nusselt number as a function of Reynolds number and particle volume concentration. Note that heat transfer enhancement for nanofluids is found compared to distilled water. Under the fixed Re, the Nusselt number is increased by about 12%

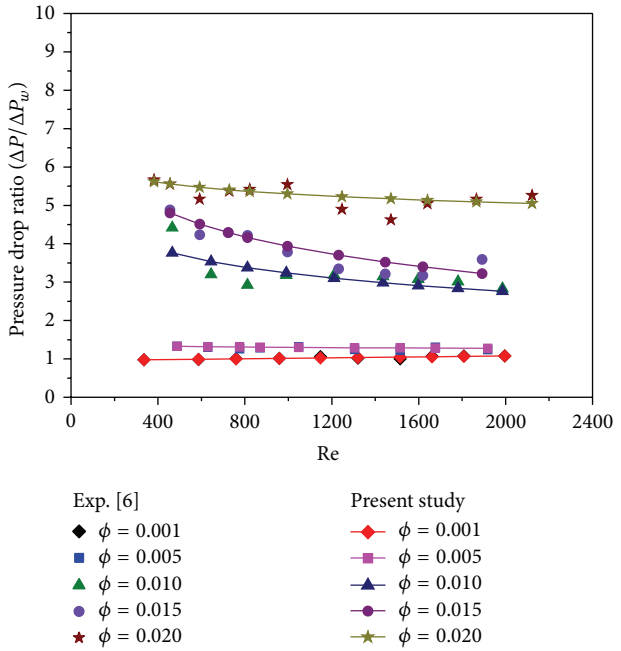

Figure 9: Variations of nanofluid-to-water ratio of pressure drop ($\Delta P/\Delta P_w$) with Reynolds number (Re) for different values of particle volume concentration (ϕ): comparison between present numerical results and experimental data [6].

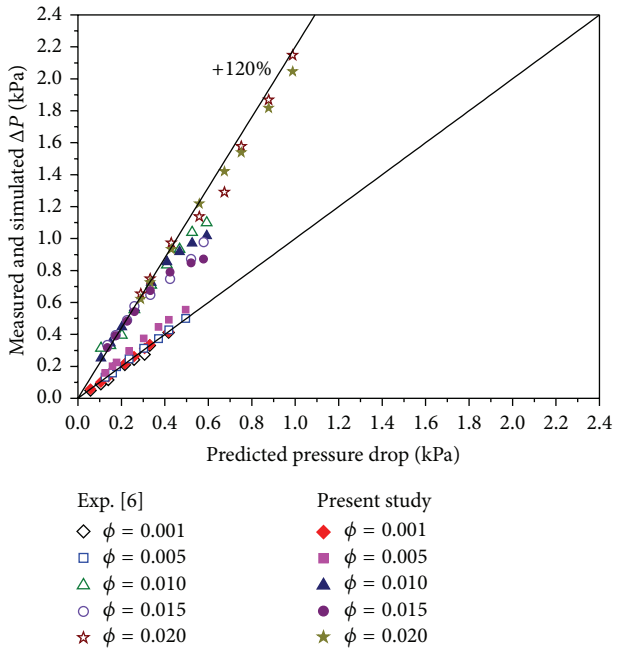

Figure 10: Pressure drop (ΔP) comparison among the present numerical results, experimental data [6], and theoretical prediction using (10) for different values of particle volume concentration (ϕ).

at ϕ = 2 vol.% in comparison to pure water, as shown in Figure 7. It is observed from Figures 6 and 7 that the addition of nanoparticles in the base fluid causes the enhancement in Nusselt number, which is due to the thermophysical properties of the nanoparticles, Brownian motion, and increased surface area [17].

Figure 8 shows the present simulated values of average Nusselt number for nanofluids compared with the experimental data [6] and the theoretical prediction using (9) [19]. As can be seen, in a laminar flow regime, the average Nusselt number in a nanofluid will always be larger than that of base fluid (water). Also, it is observed that the numerical predictions are in good agreement with the experimental measurement for water-Al_2O_3 nanofluids. However, (9) cannot predict the measured average Nusselt number well.

Figure 9 shows variations of pressure drop ratio of nanofluid to base fluid ($\Delta P/\Delta P_w$) with Reynolds number at various nanoparticle concentrations. The results show that pressure drop of nanofluids increases with increasing Reynolds number or particle volume concentration. As can be found, under a fixed Reynolds number, Re = 360, the pressure drop ratio of nanofluid to base fluid at ϕ = 2 vol.% is about 5.7. Figure 9 also shows that the numerical predictions are in good agreement with experimentally measured pressure losses.

Figure 10 shows the present simulated values of pressure loss of water-Al_2O_3 nanofluids compared with results obtained by the experiment [6] and the traditional single-phase correlation (10). In Figure 10, the predicted values of pressure losses are calculated using (10) at the same Re. At low particle concentrations (0.1 and 0.5 vol.%), the present numerical analysis shows a good agreement with the experimental data [6] and theoretical prediction (10), for pressure losses of nanofluids. However, as particle concentration is higher than 0.5 vol.%, the conventional single-phase correlation cannot predict the pressure drop of nanofluids well.

Moreover, it is noteworthy that Nusselt number and heat transfer coefficient obtained from the present numerical simulation for the nanofluid flow are in good agreement with published experimental data [6], about a 10% deviation.

4. Conclusions

In this paper, laminar flow forced convection of Al_2O_3/water nanofluid in a circular tube subjected to constant wall temperature is numerically studied. The results show that heat transfer coefficient of nanofluids increases with increasing Reynolds number or particle volume concentration. The maximum heat transfer coefficient enhancement is about 32% with 2 vol.% nanoparticle concentration for water-based Al_2O_3 nanofluid compared with that of base fluid (pure water). Increasing nanoparticle concentration leads to an increase in pressure drop for nanofluids. The maximum pressure drop ratio of nanofluid to base fluid at particle volume concentration of 2 vol.% is about 5.7. It is noteworthy that the present numerical results show a good agreement with previous published experimental data [6].

Nomenclature

C: Specific heat capacity (J/kg-K)
D: Tube diameter (inner diameter) (m)

d_p: Nanoparticle diameter (m)
h: Heat transfer coefficient (W/m^2-K)
k: Thermal conductivity (W/m-K)
L: Tube length (m)
Nu: Nusselt number
Pr: Prandtl number
Re: Reynolds number
T: Temperature (K)
T_b: Bulk (mean) temperature of the nanofluid
$T_{b,i}$: Inlet bulk (mean) temperature of the nanofluid (K)
$T_{b,o}$: Outlet bulk (mean) temperature of the nanofluid (K)
T_w: Average tube wall temperature
u: Fluid velocity (m/s).

Greek Symbols

ϕ: Nanoparticle volumetric fraction
μ: Dynamic viscosity (Pa-s)
ρ: Density (kg/m^3)
ν: Kinematic viscosity (m^2/s).

Superscript

—: Average.

Subscripts

bf: Base fluid
nf: Nanofluid
LMTD: Logarithmic mean temperature difference
m: Mean
p: Nanoparticle
w: Water or wall.

Conflict of Interests

The authors declare that there is no conflict of interests regarding the publication of this paper.

Acknowledgment

This work was supported by the National Science Council, Taiwan, under Contract NSC 102-2221-E-168-030.

References

[1] C. Pang, J. W. Lee, and Y. T. Kang, "Review on combined heat and mass transfer characteristics in nanofluids," *International Journal of Thermal Sciences*, vol. 87, pp. 49–67, 2014.

[2] B. Rimbault, C. T. Nguyen, and N. Galanis, "Experimental investigation of CuO-water nanofluid flow and heat transfer inside a microchannel heat sink," *International Journal of Thermal Sciences*, vol. 84, pp. 275–292, 2014.

[3] W. Duangthongsuk and S. Wongwises, "An experimental study on the heat transfer performance and pressure drop of TiO_2-water nanofluids flowing under a turbulent flow regime," *International Journal of Heat and Mass Transfer*, vol. 53, no. 1–3, pp. 334–344, 2010.

[4] B. C. Pak and Y. I. Cho, "Hydrodynamic and heat transfer study of dispersed fluids with submicron metallic oxide particles," *Experimental Heat Transfer*, vol. 11, no. 2, pp. 151–170, 1998.

[5] Y. Xuan and W. Roetzel, "Conceptions for heat transfer correlation of nanofluids," *International Journal of Heat and Mass Transfer*, vol. 43, no. 19, pp. 3701–3707, 2000.

[6] M. M. Heyhat, F. Kowsary, A. M. Rashidi, M. H. Momenpour, and A. Amrollahi, "Experimental investigation of laminar convective heat transfer and pressure drop of water-based Al_2O_3 nanofluids in fully developed flow regime," *Experimental Thermal and Fluid Science*, vol. 44, pp. 483–489, 2013.

[7] D. Wen and Y. Ding, "Experimental investigation into convective heat transfer of nanofluids at the entrance region under laminar flow conditions," *International Journal of Heat and Mass Transfer*, vol. 47, no. 24, pp. 5181–5188, 2004.

[8] S. Z. Heris, S. G. Etemad, and M. N. Esfahany, "Experimental investigation of oxide nanofluids laminar flow convective heat transfer," *International Communications in Heat and Mass Transfer*, vol. 33, no. 4, pp. 529–535, 2006.

[9] S. Z. Heris, M. N. Esfahany, and G. Etemad, "Numerical investigation of nanofluid laminar convective heat transfer through a circular tube," *Numerical Heat Transfer, Part A: Applications*, vol. 52, no. 11, pp. 1043–1058, 2007.

[10] S. Mirmasoumi and A. Behzadmehr, "Effect of nanoparticles mean diameter on mixed convection heat transfer of a nanofluid in a horizontal tube," *International Journal of Heat and Fluid Flow*, vol. 29, no. 2, pp. 557–566, 2008.

[11] K. V. Sharma, L. S. Sundar, and P. K. Sarma, "Estimation of heat transfer coefficient and friction factor in the transition flow with low volume concentration of Al_2O_3 nanofluid flowing in a circular tube and with twisted tape insert," *International Communications in Heat and Mass Transfer*, vol. 36, no. 5, pp. 503–507, 2009.

[12] S. Z. Heris, T. H. Nassan, S. H. Noie, H. Sardarabadi, and M. Sardarabadi, "Laminar convective heat transfer of Al_2O_3/water nanofluid through square cross-sectional duct," *International Journal of Heat and Fluid Flow*, vol. 44, pp. 375–382, 2013.

[13] Y. Xuan and Q. Li, "Investigation on convective heat transfer and flow features of nanofluids," *Journal of Heat Transfer*, vol. 125, no. 1, pp. 151–155, 2003.

[14] H. Maddah, M. Alizadeh, N. Ghasemi, and S. R. Wan Alwi, "Experimental study of Al_2O_3/water nanofluid turbulent heat transfer enhancement in the horizontal double pipes fitted with modified twisted tapes," *International Journal of Heat and Mass Transfer*, vol. 78, pp. 1042–1054, 2014.

[15] S. D. Salman, A. A. H. Kadhum, M. S. Takriff, and A. B. Mohamad, "CFD simulation of heat transfer and friction factor augmentation in a circular tube fitted with elliptic-cut twisted tape inserts," *Mathematical Problems in Engineering*, vol. 2013, Article ID 163839, 7 pages, 2013.

[16] S. D. Salman, A. A. H. Kadhum, M. S. Takriff, and A. B. Mohamad, "Heat transfer enhancement of laminar nanofluids flow in a circular tube fitted with parabolic-cut twisted tape inserts," *The Scientific World Journal*, vol. 2014, Article ID 543231, 7 pages, 2014.

[17] L. S. Sundar, M. K. Singh, I. Bidkin, and A. C. M. Sousa, "Experimental investigations in heat transfer and friction factor of magnetic Ni nanofluid flowing in a tube," *International Journal of Heat and Mass Transfer*, vol. 70, pp. 224–234, 2014.

[18] P. Fariñas Alvariño, J. M. Sáiz Jabardo, A. Arce, and M. I. Lamas Galdo, "A numerical investigation of laminar flow of a water/alumina nanofluid," *International Journal of Heat and Mass Transfer*, vol. 59, no. 1, pp. 423–432, 2013.

[19] F. P. Incroprea, D. P. DeWitt, T. L. Bergman, and A. S. Lavine, *Fundamentals of Heat and Mass Transfer*, John Wiley & Sons, 2011.